Subcellular localization of the Na^+/H^+ exchanger NHE1 in rat myocardium

KEVIN PETRECCA,[1] ROXANA ATANASIU,[1] SERGIO GRINSTEIN,[2]
JOHN ORLOWSKI,[1] AND ALVIN SHRIER[1]
[1]*Department of Physiology, McGill University, Montreal, Quebec, Canada H3G 1Y6; and* [2]*Division of Cell Biology, Hospital for Sick Children, Toronto, Ontario, Canada M5G 1X8*

Petrecca, Kevin, Roxana Atanasiu, Sergio Grinstein, John Orlowski, and Alvin Shrier. Subcellular localization of the Na^+/H^+ exchanger NHE1 in rat myocardium. *Am. J. Physiol.* 276 (*Heart Circ. Physiol.* 45): H709–H717, 1999.—The Na^+/H^+ exchanger NHE1 isoform is an integral component of cardiac intracellular pH homeostasis that is critically important for myocardial contractility. To gain further insight into its physiological significance, we determined its cellular distribution in adult rat heart by using immunohistochemistry and confocal microscopy. NHE1 was localized predominantly at the intercalated disk regions in close proximity to the gap junction protein connexin 43 of atrial and ventricular muscle cells. Significant labeling of NHE1 was also observed along the transverse tubular systems, but not the lateral sarcolemmal membranes, of both cell types. In contrast, the Na^+-K^+-ATPase α_1-subunit was readily labeled by a specific mouse monoclonal antibody (McK1) along the entire ventricular sarcolemma and intercalated disks and, to a lesser extent, in the transverse tubules. These results indicate that NHE1 has a distinct distribution in heart and may fulfill specialized roles by selectively regulating the pH microenvironment of pH-sensitive proteins at the intercalated disks (e.g., connexin 43) and near the cytosolic surface of sarcoplasmic reticulum cisternae (e.g., ryanodine receptor), thereby influencing impulse conduction and excitation-contraction coupling.

ion transporters; pH regulation; subcellular; confocal microscopy

THE CONTINUOUS contractile activity of the myocardium generates metabolic acid, which must be extruded to maintain cardiac function. This is exemplified by experimentally induced decreases in intracellular pH (pH_i), which result in marked reductions in myocardial contractility (41). The precise mechanism of this inotropic effect is not well defined but is associated with reduced myosin-ATPase activity (26), decreased ionic current through voltage-activated Na^+ and Ca^{2+} channels (21, 51, 68), diminished binding of Ca^{2+} to troponin C of the contractile apparatus (4), and reductions in gap junction conductance (55). Hence, regulation of pH_i is of critical importance for normal myocardial function.

At least three different ion transporters contribute to myocardial pH_i regulation: the Cl^-/HCO_3^- exchanger (32, 60), the Na^+-HCO_3^- cotransporter (30), and the Na^+/H^+ exchanger (NHE) (31). Of these, NHE is the main mechanism responsible for returning myocardial pH_i to the neutral range (pH_i 7.1–7.3) after an acid load (62). In mammals, at least six NHE isoforms (NHE1 to NHE6) are known to exist, and they exhibit distinct differences in their primary structures (~20–60% amino acid identity), patterns of tissue expression, membrane localization, functional properties, and physiological roles (reviewed in Refs. 43 and 61). Cardiac tissue from rats (44, 67), rabbits (58), and humans (15) expresses predominantly the NHE1 mRNA; hence, it is the main NHE isoform responsible for controlling myocardial pH_i. The heart also expresses NHE6, but it is localized to the mitochondria inner membrane (40), where it contributes primarily to matrix cation (Na^+ and indirectly Ca^{2+}) homeostasis (7).

Aside from its role in normal myocardial pH_i regulation, accumulating evidence points to NHE1 as a contributing factor in the pathophysiology of cardiac ischemia and reperfusion injuries. Metabolic alterations that create large pH gradients across the sarcolemma lead to hyperactivation of NHE1 during the early stages after ischemia and reperfusion, causing a dramatic influx of Na^+ that secondarily elevates intracellular Ca^{2+} (8, 14, 24, 47, 52). This disturbance in Ca^{2+} homeostasis is generally believed to contribute to cardiac arrhythmias, necrosis, and, eventually, contractile failure. The role of NHE1 in ischemic and reperfusion injuries, however, is most convincingly demonstrated by animal studies showing that treatment with amiloride, a relatively nonspecific inhibitor of NHE1, significantly reduces Na^+ and Ca^{2+} overload and thus has cardioprotective properties (23). Similar protective effects are obtained with amiloride analogs (9, 22, 25, 36, 39, 46, 57) and new benzoyl guanidinium compounds [e.g., HOE-694 (19, 38, 54, 66) and HOE-642 (cariporide) (53, 65)], which are more potent and selective antagonists of NHE1. The antiarrhythmic action of amiloride has also been demonstrated in human clinical studies, in which it suppressed inducible ventricular tachycardia (10) and spontaneous ventricular premature beats (37). These studies highlight the importance of examining the molecular and cellular properties of NHE1 to further understand its physiological importance in myocardial function.

NHE1 activity has been demonstrated in isolated sarcolemmal vesicles (48), although its precise location in cardiac tissue is unknown. Recent immunolocalization and subcellular fractionation studies in other cell types have provided initial indications that NHE1 is not distributed homogeneously throughout the plasma membrane. For example, although present throughout the surface membrane of adherent fibroblasts, NHE1 preferentially accumulates along the border of lamelli-

The costs of publication of this article were defrayed in part by the payment of page charges. The article must therefore be hereby marked "*advertisement*" in accordance with 18 U.S.C. Section 1734 solely to indicate this fact.

podia in close association with vinculin, talin, and F-actin, suggesting that it can be localized to specialized regions by interacting with the cytoskeleton (18). Likewise, NHE1 is restricted to the basolateral surface of polarized epithelial cells (3, 59). In this study, we examined the hypothesis that NHE1 is localized to discrete regions of the myocardial membrane. An NHE1 isoform-specific polyclonal antibody was used in conjunction with confocal immunofluorescence. The data show that NHE1 is selectively targeted to the intercalated disks and transverse tubules, suggesting that it may fulfill specialized physiological roles at these sites.

METHODS

Rat myocardial isolation. Adult Sprague-Dawley rats (250–350 g) were anesthetized with CO_2. A midline thoracotomy was performed, and the heart was rapidly removed. The preparation, containing the entire heart, was placed in a tissue bath superfused with Tyrode solution (in mmol/l: 121 NaCl, 5 KCl, 15 $NaHCO_3$, 1 Na_2HPO_4, 2.8 Na-acetate, 1 $MgCl_2$, 2.2 $CaCl_2$, and 5.5 glucose) and gassed with a 95% O_2-5% CO_2 mixture. Temperature was maintained at 37.0°C, and the pH was 7.4. The preparation was pinned down in its proper orientation and then frozen in isopentane that had been previously cooled to −40°C. The frozen preparation was then trimmed into small blocks containing the various regions under investigation. The blocks were mounted on a cryostat tissue holder using Histo Prep (Fisher Scientific), placed on the rapid-freeze stage of a Microm cryostat (Carl Zeiss), and cut into 20-μm-thick sections.

Cell culture. AP-1 cells are Na^+/H^+ exchange-deficient Chinese hamster ovary cells that were created by random chemical mutagenesis and selected by the proton-suicide technique (50). AP-1^{NHE1} cells were obtained by stable transfection of AP-1 cells with the complete coding region of the rat NHE1 isoform, as described in detail elsewhere (42). The AP-1 cells were maintained in complete α-minimal essential medium supplemented with 10% fetal bovine serum, 100 U/ml penicillin, 100 μg/ml streptomycin, and 25 mmol/l $NaHCO_3$ (pH 7.4) and incubated in a humidified atmosphere of 95% air-5% CO_2 at 37°C.

Primary antibodies. Isoform-specific polyclonal antibodies to NHE1 were raised by injecting rabbits with a fusion protein constructed with β-galactosidase of *Escherichia coli* and the last 157 amino acids of the hydrophilic (COOH-terminal) domain of the human exchanger and then affinity purified as described (18). Gap junctions were identified using a monoclonal antibody directed against residues 252–270 of the COOH terminus of the rat connexin 43 molecule (Chemicon International). The Na^+-K^+-ATPase was identified with the use of a mouse monoclonal antibody (McK1) directed against the amino acids DKKSKK near the NH_2 terminus of the rat Na^+-K^+-ATPase α_1-subunit (generously provided by Dr. Kathy Sweadner, Massachusetts General Hospital, Boston, MA) (56).

Membrane preparations. Adult Sprague-Dawley rats were anesthetized with CO_2 and killed by cervical dislocation, and the chest cavity was opened. The heart was transected below the major vessels, rinsed in PBS at 4°C, and frozen at −70°C. Rat heart membranes were prepared according to the method of Hosey et al. (20) with minor modifications. All procedures were performed at 4°C, and all solutions contained the Complete protease inhibitor cocktail (Boehringer Mannheim, Mannheim, Germany). Hearts were minced, diluted in 10 volumes of Tris-EDTA (TE) buffer (10 mmol/l Tris and 1 mmol/l EDTA, pH 7.4), and homogenized three times (10 s each) with a Brinkman Polytron (Brinkman Instruments, Westbury, NY) at a setting of 9. Nuclei and cell debris were pelleted by centrifugation at 1,000 *g* for 10 min. The pellet was rehomogenized in TE buffer and the centrifugation step repeated. The supernatants from both low-speed spins were pooled and centrifuged at 30,000 *g* for 30 min. To depolymerize the actin, the pellet was resuspended in TE containing 0.6 mol/l KI and incubated on ice for 30 min. After centrifugation at 30,000 *g* for 30 min, the resulting pellet was resuspended in TE and washed two times to completely remove the KI. The final pellet was solubilized by boiling in TE containing 1% SDS, and the insoluble material was centrifuged at 13,000 *g* for 30 min.

Confluent AP-1 cells were washed three times with PBS, scraped off the plates, lysed in radioimmunoprecipitation assay buffer (150 mmol/l NaCl, 20 mmol/l Tris·HCl, 0.1% SDS, 0.5% deoxycholate, and 1% Triton X-100, pH 8.0) supplemented with protease inhibitor cocktail, and spun at 2,400 *g* for 5 min. The supernatant was collected as a crude membrane fraction.

The protein concentration of all of the membrane preparations was measured using the Bio-Rad DC Protein Assay kit. Solubilized membranes were aliquoted and stored at −70°C until use.

SDS-PAGE and immunoblotting. Samples containing AP-1 (20 μg protein) and rat heart (40 μg protein) membranes were resolved on 10% SDS-polyacrylamide gels and electrophoretically transferred to PolyScreen polyvinylidene difluoride (PVDF) membranes (NEN, Boston, MA). After transfer, the PVDF membranes were quenched in PBS containing 5% nonfat dry milk and 0.1% wt/vol Tween 20 for 1 h. Polyclonal NHE1 antiserum was added to a final dilution of 1:5,000, and the incubation was allowed to proceed for another 2 h at room temperature. The membranes were further incubated with goat anti-rabbit IgG conjugated with horseradish peroxidase (New England BioLabs) for 1 h at room temperature, and the labeled proteins were detected by enhanced chemiluminescence using a Western blotting detection kit (Amersham).

To demonstrate the specificity of the immunoreactivity, duplicate samples were submitted to the same protocol except that the primary antibody was preincubated for 1 h with the NHE1 fusion protein (1 μg/ml final concentration) used to generate the antiserum.

Immunohistochemistry. Cryostat sections (20 μm thick) prepared from frozen hearts were mounted onto slides and air-dried at room temperature for 1 h. After the sections were permeabilized and blocked with 0.2% Triton X-100–0.5% BSA in PBS, they were incubated for 2 h at room temperature with primary antibody diluted in 0.2% Triton X-100–0.5% BSA in PBS. After being washed three times in PBS (pH 7.2), the sections were incubated with secondary antibody (Texas Red-conjugated goat anti-rabbit IgG or FITC-conjugated goat anti-mouse IgG, Jackson Immunoresearch Laboratories) diluted in 0.2% Triton X-100–0.5% BSA in PBS for 1 h at room temperature and then rinsed three times in PBS. Sections were then mounted using Immuno Flore (ICN). Controls include omission of the primary antibodies directed against NHE1, connexin 43, and Na^+-K^+-ATPase and NHE1 antibody competition with the fusion protein that the antibody was generated against.

Immunocytochemistry. Cells grown on coverslips were fixed in 1% paraformaldehyde for 15 min at room temperature and then rinsed three times in PBS (pH 7.2). Cells were then permeabilized and blocked by incubation in 0.2% Triton X-100–0.5% BSA in PBS for 30 min at room temperature. Cells were subsequently rinsed in PBS and incubated with appropriately diluted primary antibody in 0.2% Triton X-100–

0.5%BSA in PBS for 1 h at room temperature. After being rinsed three times in PBS, cells were incubated in secondary antibody (Texas Red-conjugated goat anti-rabbit IgG, Jackson Immunoresearch Laboratories) diluted in 0.2% Triton X-100–0.5%BSA in PBS for 1 h at room temperature and then rinsed three times in PBS. Sections were then mounted using Immuno Flore (ICN).

Confocal laser scanning microscopy. For confocal microscopy, sections from nine hearts were analyzed for immunolocalization of NHE1. An additional four hearts were analyzed for localization of Na^+-K^+-ATPase and colocalization of NHE1 and connexin 43. All imaging was performed using a Zeiss LSM 410 inverted confocal microscope. Texas Red-conjugated secondary antibodies were excited with a helium/neon (543 nm) laser and were imaged on a photomultiplier after passage through FT560 and LP590 filter sets. FITC-conjugated secondary antibodies were imaged by exciting the sample with a 488-nm line from an argon/krypton laser, and the resulting fluorescence was collected on a photomultiplier after passage through FT510 and BP515–540 filter sets. All images were printed on a Kodak XLS8300 high-resolution (300 dpi) printer. Optical sections were taken using a ×25, 0.8 NA objective (optical thickness 3.1 μm) or a ×63, 1.4 NA objective (optical thickness 1.0 μm). The imaging parameters, including contrast and brightness and acquisition times, were similar for all positive and negative experiments within Figs. 2–7. The data presented in this study are identical to, and representative of, all experiments.

RESULTS

Myocardial distribution of Na^+/H^+ exchangers. To determine the cellular location of NHE1 in the intact rat myocardium, we used confocal immunofluorescence microscopy and an isoform-specific anti-human NHE1 antibody that has been successfully used for the detection of NHE1 by immunocytochemistry and Western blotting (17, 18). Rat NHE1 has a high degree of sequence similarity with human NHE1 and was therefore anticipated to react with the anti-human NHE1 antibody. Figure 1 shows the specificity of the antibody as determined by immunoblotting of protein extracts from NHE1-transfected fibroblasts and heart tissue; a prominent immunoreactive band of ~110 kDa (fully glycosylated form) and smaller amounts of dimerized (~200 kDa) and nonglycosylated (~90 kDa) forms were observed in crude cell extracts from stably transfected AP-1 cells overexpressing rat NHE1 (AP-1^{NHE1}, Fig. 1, *lane 1*), consistent with previous reports (12, 17). In comparison, enriched membranes isolated from rat heart (Fig. 1, *lane 2*) contained smaller amounts of the fully glycosylated NHE1 and minor amounts of the dimerized form, but the nonglycosylated protein was absent or below the detection sensitivity of the antibody. These bands could be competed off by incubation of the primary antibody with excess soluble NHE1 fusion protein (Fig. 1, *lanes 3* and *4*), demonstrating the specificity of this detection system. Other smaller, fainter bands were also detected in extracts from AP-1^{NHE1} cells and heart tissue. Some of these were competed off by excess soluble NHE1 fusion protein, suggesting that they may be proteolytic products of NHE1 that arose during tissue processing. Other bands were neither consistently observed between different

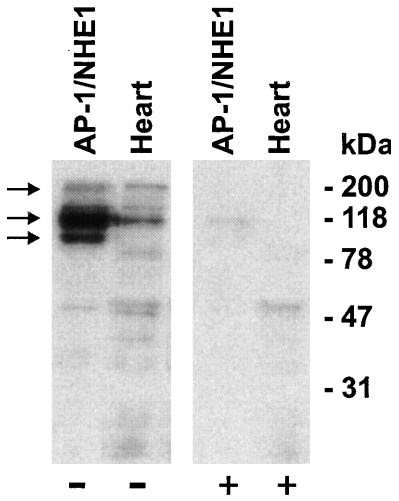

Fig. 1. Detection of rat Na^+/H^+ exchanger NHE1 protein in membrane preparations from AP-1 cells and rat heart. Membrane fractions were prepared from AP-1 cells stably transfected with rat NHE1 (AP-1^{NHE1}) and rat hearts as described in METHODS. Proteins were resolved by SDS-PAGE and then detected by immunoblotting. Blots were preincubated with NHE1 antiserum (final dilution 1:5,000) either in absence (−) or presence (+) of soluble NHE1 fusion protein (final concentration 1 μg/ml) used to generate antiserum, followed by incubation with goat anti-rabbit IgG conjugated with horseradish peroxidase. Labeled proteins were detected by enhanced chemiluminescence. Positions of monomeric [nonglycosylated (~90 kDa) and fully glycosylated (~110 kDa)] and dimeric (~200 kDa) forms of NHE1 are indicated by arrows at *left*; positions of prestained molecular mass markers are indicated at *right*.

experiments nor effectively quenched by the soluble NHE1 fusion protein and, hence, are likely of nonspecific origin. Further analysis showed significant labeling of NHE1 throughout the cell surface and, to a lesser extent, in the perinuclear region of transfected AP-1^{NHE1} cells (Fig. 2*A*), whereas in nontransfected AP-1 cells, surface-associated and perinuclear immunofluorescence was extremely faint and diffuse (Fig. 2*B*), in agreement with an earlier report using whole cells (18). These initial experiments suggested that the fluorescence pattern generated by this antibody is a valid indicator of the distribution of NHE1 in cells and tissues.

Immunolabeling of longitudinal sections of rat ventricle revealed that NHE1 accumulated preferentially at the intercalated disk region and less intensely along parallel lines corresponding to the transverse tubular system (Fig. 3, *A* and *B*). In contrast, no labeling was

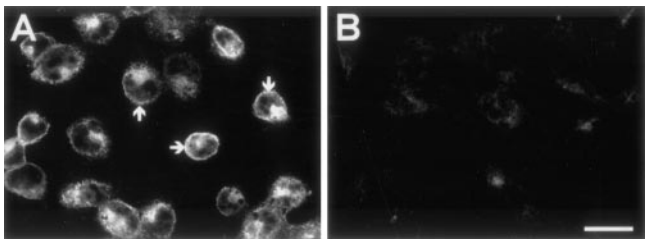

Fig. 2. Expression of NHE1 protein in AP-1 cells. *A*: immunofluorescence image of AP-1^{NHE1} cells incubated with anti-NHE1 antibody. Arrows indicate plasma membrane labeling. *B*: immunofluorescence image of nontransfected AP-1 cells incubated with anti-NHE1 antibody. Bar, 20 μm.

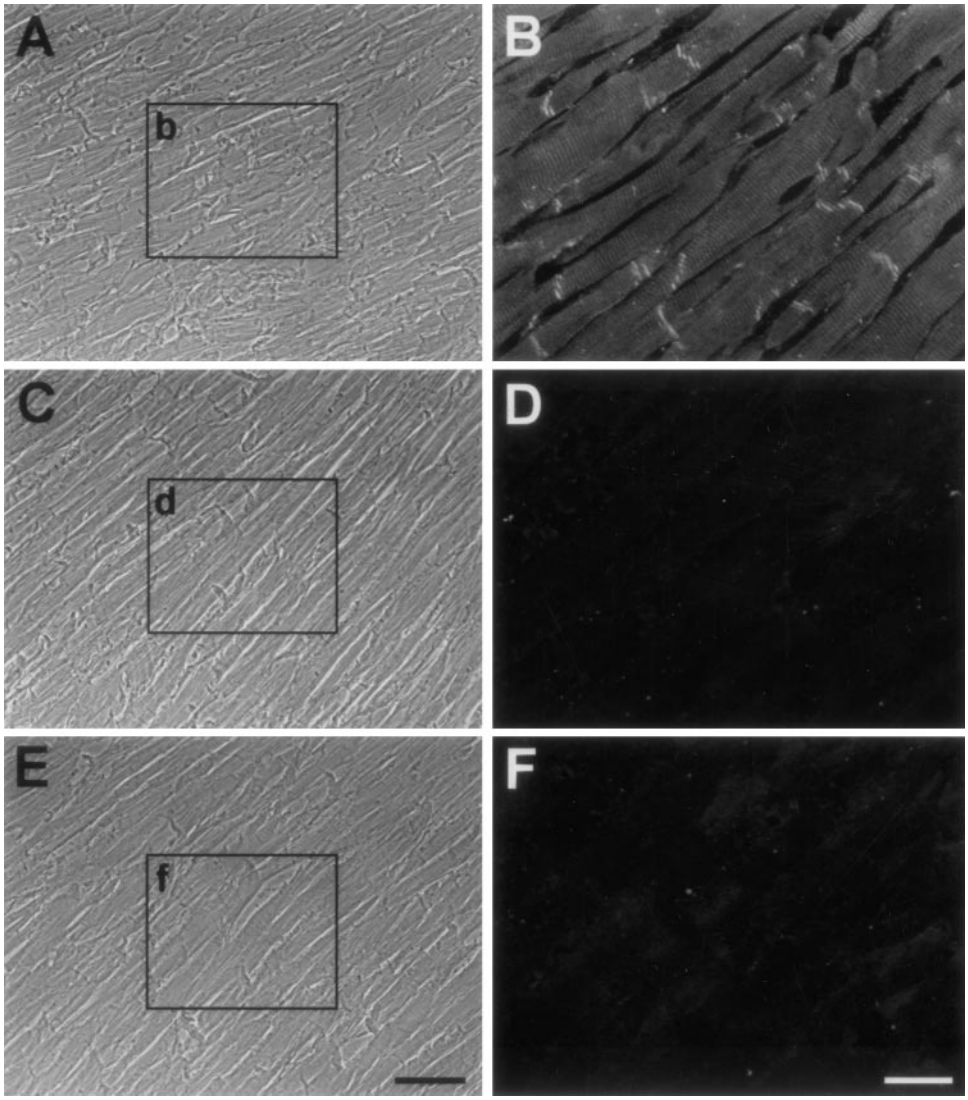

Fig. 3. Expression of NHE1 in rat heart. *A*: transmitted light image of a 20-μm-thick section of ventricle. *B*: immunofluorescence image of ventricular section in *A* (*inset b*) incubated with anti-NHE1 antibody followed by Texas Red-conjugated goat anti-rabbit IgG. *C*: transmitted light image of a 20-μm-thick section of ventricle. *D*: immunofluorescence image of ventricular section in *C* (*inset d*) incubated in presence of Texas Red-conjugated goat anti-rabbit IgG only. *E*: transmitted light image of a 20-μm-thick section of ventricle. *F*: immunofluorescence image of ventricular section in *E* (*inset f*) incubated in presence of anti-NHE1 antibody and NHE1 fusion protein that primary antibody was generated against followed by Texas Red-conjugated goat anti-rabbit IgG. Magnification in *A*, *C*, and *E* is identical; bar in *E*, 62.5 μm. Magnification in *B*, *D*, and *F* is identical; bar in *F*, 25 μm.

detected along the lateral sarcolemma regardless of the optical plane. Control sections treated with the secondary antibody alone (Fig. 3, *C* and *D*) or with both the primary and Texas Red-conjugated secondary antibodies in the presence of the NHE1 fusion protein used to generate the antibody (Fig. 3, *E* and *F*) gave no signals, confirming the specificity of the immunoreactivity. The lack of signal in the presence of competing soluble NHE1 antigen also indicates that the minor nonspecific bands detected in the Western blot were not a contributing factor to the immunofluorescence signal. Similar results were obtained for both ventricular (Fig. 4, *A* and *B*) and atrial (Fig. 4, *C* and *D*) tissue shown at two higher magnifications.

To establish the validity of these observations, we examined the locations of two other previously characterized proteins in cardiac tissue: connexin 43, which is confined to gap junctions at the intercalated disks (2), and the Na^+-K^+-ATPase α_1-subunit, which is distributed along the surface sarcolemma and transverse tubules (35, 56). As shown in Fig. 5 at low (Fig. 5, *A* and *B*) and high (Fig. 5*C*) magnification, labeling longitudinal sections of rat ventricular muscle with a mouse monoclonal antibody directed against rat connexin 43 revealed clusters of transversely oriented gap junctions at the intercalated disks, in agreement with other studies (2). Labeling was not detected in control sections treated with the FITC-conjugated secondary antibody alone (Fig. 5*D*). However, when ventricular tissue was labeled with a specific monoclonal antibody (McK1) raised against the rat Na^+-K^+-ATPase α_1-subunit, it showed a more uniform distribution along the entire sarcolemma and intercalated disk region (Fig. 6, *A* and *B*). Less prominent labeling is also observed in the transverse tubules at higher magnifications (Fig. 6*C*). Again, control sections treated with the secondary antibody alone (Fig. 6*D*) were negative. These latter results are consistent with reports of other studies in which the same anti-Na^+-K^+-ATPase α_1-antibody was used (35, 56). Dual labeling experiments of NHE1 (Fig. 7*A*) and connexin 43 (Fig. 7*B*) confirm that they are colocalized to the intercalated disk regions (Fig. 7*C*), although they do not appear to occupy the same sites.

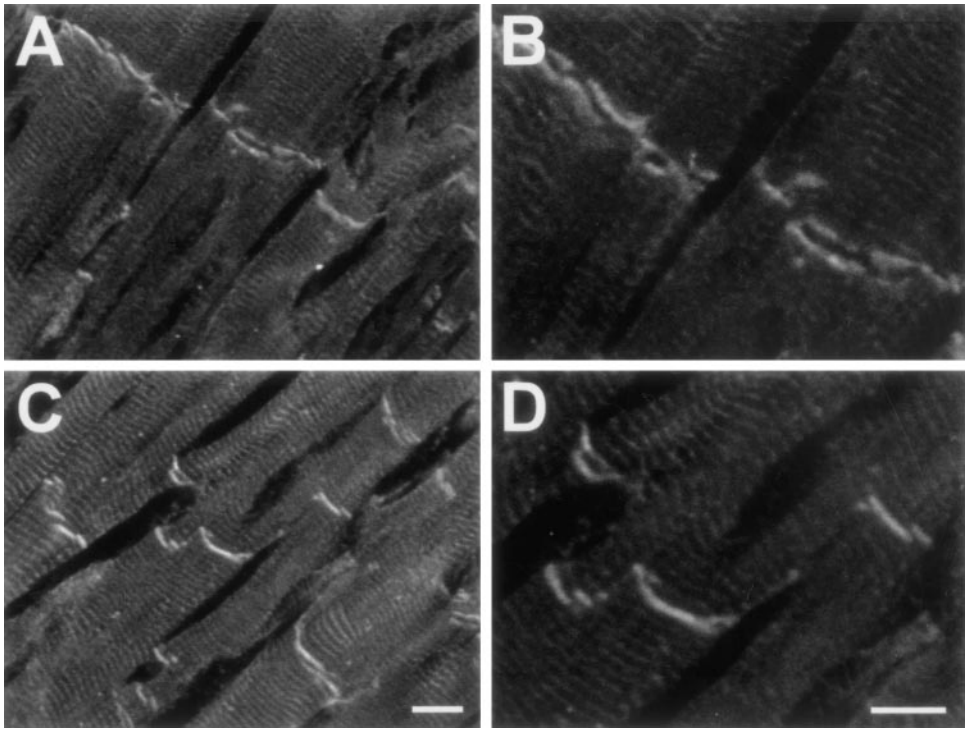

Fig. 4. Comparison of NHE1 protein expression in ventricular and atrial myocardium. *A*: immunofluorescence image of ventricular tissue incubated in presence of anti-NHE1 antibody. *B*: high-magnification image of *A*. *C*: immunofluorescence image of atrial tissue incubated in presence of anti-NHE1 antibody. *D*: high-magnification image of *C*. Magnification in *A* and *C* is identical; bar in *C*, 10 μm. Magnification in *B* and *D* is identical; bar in *D*, 10 μm.

DISCUSSION

NHE1 is localized in rat cardiac myocytes at intercalated disks and transverse tubules. Biochemical studies have indicated that Na^+/H^+ exchanger activity (i.e., NHE1 isoform) is present in isolated sarcolemmal vesicles (48). By using an isoform-specific anti-NHE1 polyclonal antibody and confocal immunofluorescence microscopy, we have shown that NHE1 is preferentially localized at the intercalated disk regions and transverse tubular system of adult rat atrial and ventricular muscle cells. In this study, the specificity of immunolabeling in rat heart is demonstrated by the lack of a detectable signal in the presence of a competing soluble form of the NHE1 antigen added during incubation with the primary antibody and by the absence of a signal in the presence of secondary antibody alone.

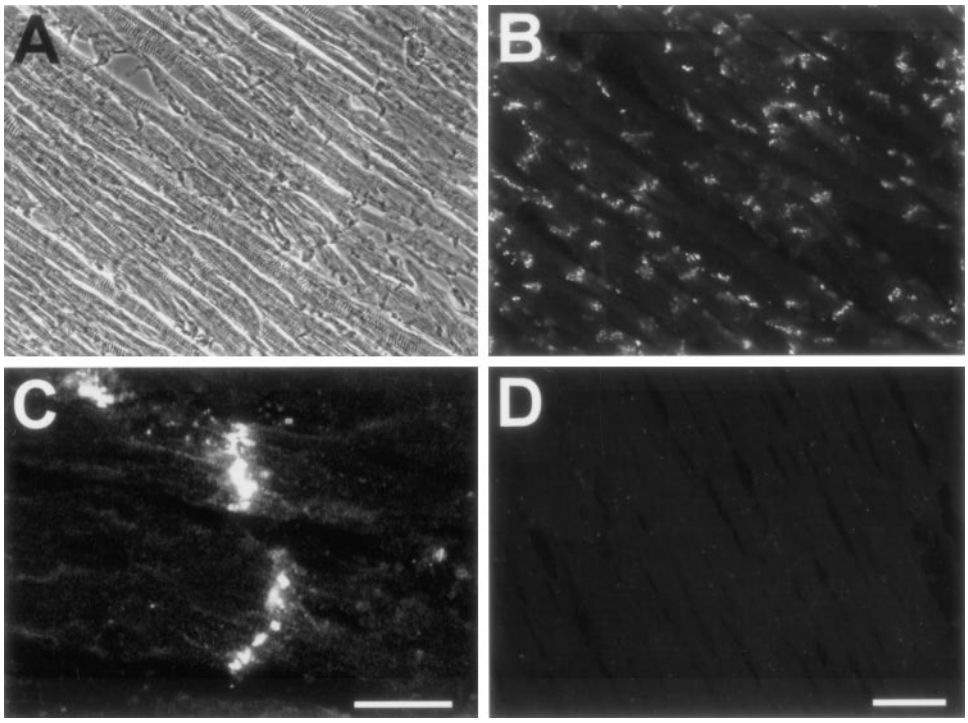

Fig. 5. Connexin 43 protein expression in ventricular myocardium. *A*: transmitted light image of a 20-μm-thick section of ventricle. *B*: low magnification of an immunofluorescence image of ventricular section in *A* incubated with anti-connexin 43 antibody followed by Texas Red-conjugated goat anti-mouse IgG. *C*: higher magnification of an immunofluorescence image of a ventricular section incubated with anti-connexin 43 antibody followed by Texas Red-conjugated goat anti-mouse IgG. Bar, 10 μm. *D*: immunofluorescence image of a ventricular section incubated with Texas Red-conjugated goat anti-mouse IgG only at a magnification identical to that in *A* and *B*; bar, 50 μm.

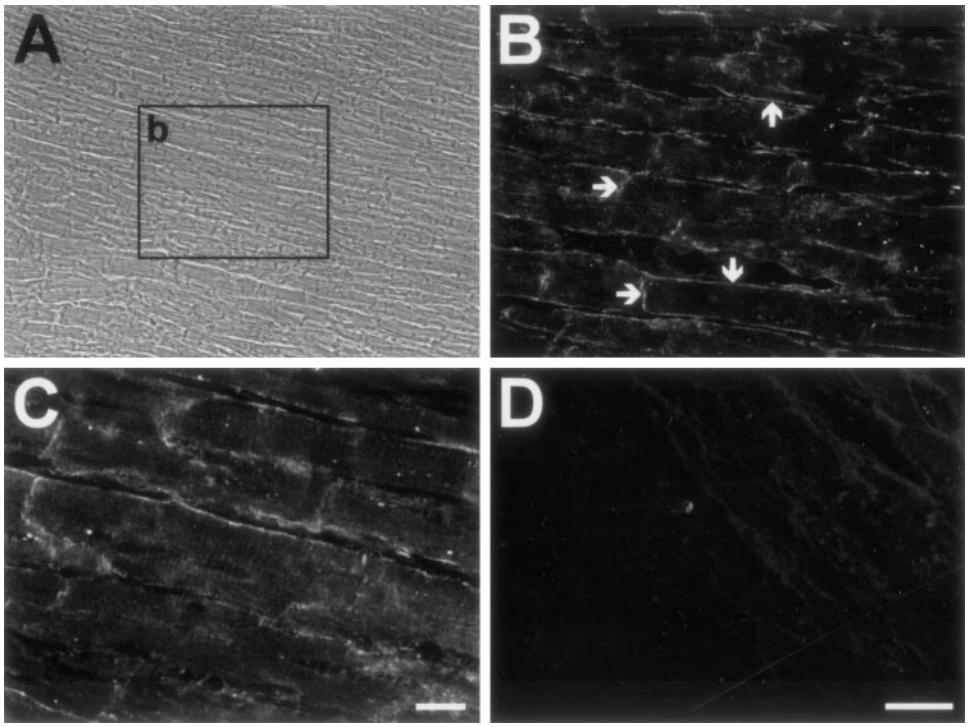

Fig. 6. Na^+-K+-ATPase protein expression in ventricular myocardium. *A*: transmitted light image of a 20-μm-thick section of ventricle. *B*: immunofluorescence image of ventricular section in *A* (*inset b*) incubated with McK1 followed by Texas Red-conjugated goat anti-mouse IgG. Vertical arrows indicate lateral membrane labeling; horizontal arrows indicate labeling at intercalated disk region. *C*: immunofluorescence image of a 20-μm-thick section of ventricle incubated with McK1 followed by Texas Red-conjugated goat anti-mouse IgG at higher magnification. Bar, 10 μm. *D*: immunofluorescence image of a ventricular section incubated with Texas Red-conjugated goat anti-mouse IgG only. Magnification in *B* and *D* is identical; bar in *D*, 25 μm.

Taken together, these data strongly suggest that the observed immunolabeling represents localization of NHE1 protein to the intercalated disks and transverse tubules.

Immunolabeling of NHE1 at the intercalated disks appears more intense than that of the transverse tubular system. This could represent selective clustering and higher densities of NHE1 protein per unit area of membrane, analogous to the preferential accumulation of NHE1 along the border of lamellipodia in fibroblasts (18). Alternatively, the intense signals may reflect increased membrane surface area due to the infolding of the sarcolemma at the intercalated disks (45).

Unexpectedly, NHE1 was not observed along the lateral sarcolemma. The possibility that this membrane compartment was inaccessible to antibodies under the given experimental conditions was excluded by our ready detection of the Na^+-K^+-ATPase α_1-subunit in the lateral sarcolemma. Whereas the absence of labeling of NHE1 may reflect a level of abundance that is below the detection sensitivity of the antibody, the data are more readily explained by the selective targeting of NHE1 to the intercalated disk and transverse tubular membranes. This distribution differs somewhat from that of the Na^+/Ca^{2+} exchanger, which, like the Na^+-K^+-ATPase α_1-subunit, is present throughout the sarcolemma, the transverse tubules, and the intercalated disks of isolated ventricular myocytes from adult guinea pig and rat hearts (16, 27). Other pH regulatory transporters also appear to exhibit preferential membrane targeting in heart. An antibody that recognizes both the AE1 and AE3 isoforms of the Cl^-/HCO_3^- exchanger revealed that they accumulated mainly at the lateral sarcolemma and transverse tubules of isolated adult rat ventricular myocytes (49), although it was not established whether these isoforms were differentially targeted to these membrane surfaces. The location of the other major cardiac pH regulatory protein, the Na^+-HCO_3^- cotransporter, is currently unknown. Thus the distribution of the NHE1 isoform in cardiac myocytes appears distinct from that of other known exchangers and pumps. The mechanisms responsible for this differential membrane localization are unknown.

Functional implications for subcellular localization of NHE1 in heart. The immunofluorescence data revealed that NHE1 accumulates at the intercalated disks in close proximity to the predominant cardiac gap junction protein connexin 43, which suggests that a functional relationship may exist between the two proteins. It is well known that small changes in pH_i within the physiological range regulate gap junction conductance (55, 63). The molecular basis for this phenomenon is not fully understood, but electrophysiological studies have shown that decreasing pH_i reduces the open probability of individual cardiac gap junction channels (5). Recent structural studies have implicated His95 (11) and the carboxy tail (33) of connexin 43 as critical components involved in "H^+ gating" of the cardiac gap junction. Thus it is reasonable to suggest that neighboring NHEs may play a role in this regulation. Indeed, pretreatment of rat neonatal paired cardiomyocytes with amiloride (1 mmol/l), a nonselective inhibitor of NHE1, enhanced the inhibitory effects of acidic pH_i on conductance of gap junctions, presumably by retarding extrusion of protons (13). The caveat to this study is that the effects of

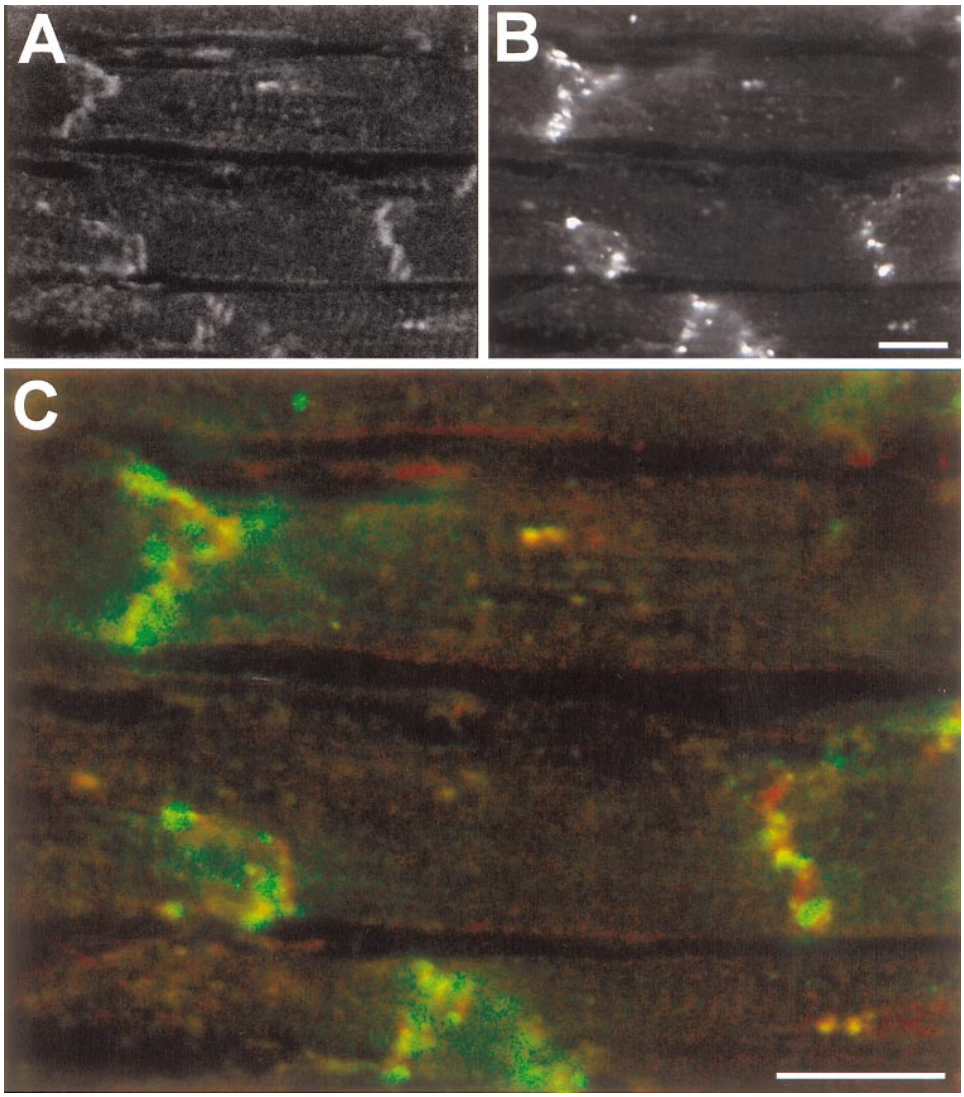

Fig. 7. Colocalization of NHE1 and connexin 43 protein expression in ventricular myocardium. *A*: immunofluorescence image of ventricular tissue incubated in presence of anti-NHE1 antibody. *B*: immunofluorescence image of ventricular tissue (same region as in *A*) incubated in presence of anti-connexin 43 antibody. Magnification in *A* and *B* is identical; bar in *B*, 10 μm. *C*: overlay of *A* and *B*. NHE1 protein expression is visible as red labeling; connexin 43 protein expression is visible as green labeling. Bar, 10 μm.

amiloride could have been secondary to inhibition of other transporters and channels (29), thus making it difficult to firmly establish a functional link between NHE1 activity and gap junction conductance. Nevertheless, the data are consistent with the hypothesis that the high density of NHE1 in the intercalated disk region serves to regulate the pH_i environment of gap junctions, particularly connexin 43, thereby influencing intercellular communication.

Aside from NHE1, other ion transport proteins are also concentrated at the intercalated disk region of cardiac myocytes, such as voltage-gated Na^+ channels (H1 subtype) (6), voltage-gated K^+ channels (1, 34), and inositol 1,4,5-trisphosphate Ca^{2+} release channels (i.e., IP_3 receptors) (28). Whether these ion channels are similarly influenced by physiologically relevant changes in pH_i is unknown.

Likewise, it is attractive to speculate that the presence of NHE1 along the transverse tubules is functionally coupled to the rapid release of Ca^{2+} by the sarcoplasmic reticulum Ca^{2+} release channel (i.e., ryanodine receptor), which is highly pH_i-sensitive (64); a minor cytosolic acidification decreases the rate of Ca^{2+} release, which is directly involved in triggering the contractile process.

In conclusion, the data show that NHE1 is specifically targeted to distinct regions of cardiac myocytes. We speculate that NHE1 may fulfill specialized roles in the heart by selectively regulating the pH microenvironment of pH-sensitive proteins at the intercalated disks (e.g., connexin 43) and near the cytosolic surface of sarcoplasmic reticulum cisternae (e.g., ryanodine receptor), thereby influencing impulse conduction and excitation-contraction coupling.

This work was funded by the Medical Research Council of Canada. S. Grinstein is an International Scholar of the Howard Hughes Medical Institute and is cross-appointed to the Department of Biochemistry of the University of Toronto. J. Orlowski is supported by a Scientist Award from the Medical Research Council of Canada.

K. Petrecca is supported by a studentship from the Fonds pour la Formation de Chercheurs et l'Aide à la Recherche (FCAR).

Address for reprint requests: J. Orlowski, Dept. of Physiology, McGill Univ., McIntyre Medical Science Bldg., 3655 Drummond St., Montreal, Quebec, Canada H3G 1Y6.

Received 22 July 1998; accepted in final form 2 October 1998.

REFERENCES

1. **Barry, D. M., J. S. Trimmer, J. P. Merlie, and J. M. Nerbonne.** Differential expression of voltage-gated K^+ channel subunits in adult rat heart. Relation to functional K^+ channels? *Circ. Res*. 77: 361–369, 1995.
2. **Beyer, E. C., J. Kistler, D. L. Paul, and D. A. Goodenough.** Antisera directed against connexin43 peptides react with a 43-kD protein localized to gap junctions in myocardium and other tissues. *J. Cell Biol*. 108: 595–605, 1989.
3. **Biemesderfer, D., R. F. Reilly, M. Exner, P. Igarashi, and P. S. Aronson.** Immunocytochemical characterization of Na^+-H^+ exchanger isoform NHE-1 in rabbit kidney. *Am. J. Physiol*. 263 (*Renal Fluid Electrolyte Physiol*. 32): F833–F840, 1992.
4. **Blanchard, E. M., and R. J. Solaro.** Inhibition of the activation and troponin calcium binding of dog cardiac myofibrils by acidic pH. *Circ. Res*. 55: 382–391, 1984.
5. **Burt, J. M., and D. C. Spray.** Single channel events and gating behavior of the cardiac gap junction channel. *Proc. Natl. Acad. Sci. USA* 85: 3431–3434, 1988.
6. **Cohen, S. A.** Immunocytochemical localization of rH1 sodium channel in adult rat heart atria and ventricle. Presence in terminal intercalated disks. *Circulation* 94: 3083–3086, 1996.
7. **Crompton, M., and I. Heid.** The cycling of calcium, sodium, and protons across the inner membrane of cardiac mitochondria. *Eur. J. Biochem*. 91: 599–608, 1978.
8. **Duff, H. J.** Clinical and in vivo antiarrhythmic potential of sodium-hydrogen exchange inhibitors. *Cardiovasc. Res*. 29: 189–193, 1995.
9. **Duff, H. J., C. E. Brown, E. J. Cragoe, Jr., and M. Rahmberg.** Antiarrhythmic activity of amiloride: mechanisms. *J. Cardiovasc. Pharmacol*. 17: 879–888, 1991.
10. **Duff, H. J., L. B. Mitchell, K. M. Kavanagh, D. E. Manyari, A. M. Gillis, and D. G. Wyse.** Amiloride: antiarrhythmic and electrophysiological actions in patients with sustained ventricular tachycardia. *Circulation* 79: 1257–1263, 1989.
11. **Ek, J. F., M. Delmar, R. Perzova, and S. M. Taffet.** Role of histidine 95 on the pH gating of the cardiac gap junction protein connexin43. *Circ. Res*. 74: 1058–1064, 1994.
12. **Fafournoux, P., J. Noël, and J. Pouysségur.** Evidence that Na^+/H^+ exchanger isoforms NHE1 and NHE3 exist as stable dimers in membranes with a high degree of specificity for homodimers. *J. Biol. Chem*. 269: 2589–2596, 1994.
13. **Firek, L., and R. Weingart.** Modification of gap junction conductance by divalent cations and protons in neonatal rat heart cells. *J. Mol. Cell. Cardiol*. 27: 1633–1643, 1995.
14. **Fliegel, L., and J. R. B. Dyck.** Molecular biology of the cardiac sodium/hydrogen exchanger. *Cardiovasc. Res*. 29: 155–159, 1995.
15. **Fliegel, L., J. R. B. Dyck, H. Wang, C. Fong, and R. S. Haworth.** Cloning and analysis of the human myocardial Na^+/H^+ exchanger. *Mol. Cell. Biochem*. 125: 137–143, 1993.
16. **Frank, J. S., G. Mottino, D. Reid, R. S. Molday, and K. D. Philipson.** Distribution of the Na^+-Ca^{2+} exchange protein in mammalian cardiac myocytes: An immunofluorescence and immunocolloidal gold-labeling study. *J. Cell Biol*. 117: 337–345, 1992.
17. **Fukushima, T., T. K. Waddell, S. Grinstein, G. G. Goss, J. Orlowski, and G. P. Downey.** Na^+/H^+ exchange activity during phagocytosis in human neutrophils: role of Fcgamma receptors and tyrosine kinases. *J. Cell Biol*. 132: 1037–1052, 1996.
18. **Grinstein, S., M. Woodside, T. K. Waddell, G. P. Downey, J. Orlowski, J. Pouysségur, D. C. P. Wong, and J. K. Foskett.** Focal localization of the NHE-1 isoform of the Na^+/H^+ antiport: assessment of effects on intracellular pH. *EMBO J*. 12: 5209–5218, 1993.
19. **Harper, I. S., J. M. Bond, E. Chacon, J. M. Reece, B. Herman, and J. J. Lemasters.** Inhibition of Na^+/H^+ exchange preserves viability, restores mechanical function, and prevents the pH paradox in reperfusion injury to rat neonatal myocytes. *Basic Res. Cardiol*. 88: 430–442, 1993.
20. **Hosey, M. M., and J. Z. Fields.** Quantitative and qualitative differences in muscarinic cholinergic receptors in embryonic and newborn chick hearts. *J. Biol. Chem*. 256: 6395–6399, 1981.
21. **Irisawa, H., and R. Sato.** Intra- and extracellular actions of proton on the calcium current of isolated guinea pig ventricular cells. *Circ. Res*. 59: 348–355, 1986.
22. **Kaplan, S. H., H. Yang, D. E. Gilliam, J. Shen, J. J. Lemasters, and W. E. Cascio.** Hypercapnic acidosis and dimethyl amiloride reduce reperfusion induced cell death in ischaemic ventricular myocardium. *Cardiovasc. Res*. 29: 231–238, 1995.
23. **Karmazyn, M.** Amiloride enhances postischemic ventricular recovery: possible role of Na^+/H^+ exchange. *Am. J. Physiol*. 255 (*Heart Circ. Physiol*. 24): H608–H615, 1988.
24. **Karmazyn, M., and M. P. Moffat.** Role of Na^+/H^+ exchange in cardiac physiology and pathophysiology: mediation of myocardial reperfusion injury by the pH paradox. *Cardiovasc. Res*. 27: 915–924, 1993.
25. **Karmazyn, M., M. Ray, and J. V. Haist.** Comparative effects of Na^+/H^+ exchange inhibitors against cardiac injury produced by ischemia/reperfusion, hypoxia/reoxygenation, and the calcium paradox. *J. Cardiovasc. Pharmacol*. 21: 172–178, 1993.
26. **Kentish, J. C., and W. G. Nayler.** The influence of pH on the Ca^{2+}-regulated ATPase of cardiac and white skeletal myofibrils. *J. Mol. Cell. Cardiol*. 11: 611–617, 1979.
27. **Kieval, R. S., R. J. Bloch, G. E. Lindenmayer, A. Ambesi, and W. J. Lederer.** Immunofluorescence localization of the Na-Ca exchanger in heart cells. *Am. J. Physiol*. 263 (*Cell Physiol*. 32): C545–C550, 1992.
28. **Kijima, Y., A. Saito, T. L. Jetton, M. A. Magnuson, and S. Fleischer.** Different intracellular localization of inositol 1,4,5-trisphosphate and ryanodine receptors in cardiomyocytes. *J. Biol. Chem*. 268: 3499–3506, 1993.
29. **Kleyman, T. R., and E. J. Cragoe, Jr.** Amiloride and its analogs as tools in the study of ion transport. *J. Membr. Biol*. 105: 1–21, 1988.
30. **Lagadic-Gossmann, D., K. J. Buckler, and R. D. Vaughan-Jones.** Role of bicarbonate in pH recovery from intracellular acidosis in the guinea-pig ventricular myocyte. *J. Physiol. (Lond.)* 458: 361–384, 1992.
31. **Lazdunski, M., C. Frelin, and P. Vigne.** The sodium/hydrogen exchange system in cardiac cells: its biochemical and pharmacological properties and its role in regulating internal concentrations of sodium and internal pH. *J. Mol. Cell. Cardiol*. 17: 1029–1042, 1985.
32. **Liu, S., D. Piwnica-Worms, and M. Lieberman.** Intracellular pH regulation in cultured embryonic chick heart cells. Na^+-dependent Cl^-/HCO_3^- exchange. *J. Gen. Physiol*. 96: 1247–1269, 1990.
33. **Liu, S., S. Taffet, L. Stoner, M. Delmar, M. L. Vallano, and J. Jalife.** A structural basis for the unequal sensitivity of the major cardiac and liver gap junctions to intracellular acidification: the carboxyl tail length. *Biophys. J*. 64: 1422–1433, 1993.
34. **Mays, D. J., J. M. Foose, L. H. Philipson, and M. M. Tamkun.** Localization of the Kv1.5 K^+ channel protein in explanted cardiac tissue. *J. Clin. Invest*. 96: 282–292, 1995.
35. **McDonough, A. A., Y. Zhang, V. Shin, and J. S. Frank.** Subcellular distribution of the sodium pump isoform subunits in mammalian cardiac myocytes. *Am. J. Physiol*. 270 (*Cell Physiol*. 39): C1221–C1227, 1996.
36. **Moffat, M. P., and M. Karmazyn.** Protective effects of the potent Na/H exchange inhibitor methylisobutyl amiloride against post-ischemic contractile dysfunction in rat and guinea-pig hearts. *J. Mol. Cell. Cardiol*. 25: 959–971, 1993.
37. **Myers, M.** Diuretic therapy and ventricular arrhythmias in persons 65 years of age and older. *Am. J. Cardiol*. 65: 599–603, 1990.
38. **Myers, M. L., and M. Karmazyn.** Improved cardiac function after prolonged hypothermic ischemia with the Na^+/H^+ exchange inhibitor HOE 694. *Ann. Thorac. Surg*. 61: 1400–1406, 1996.
39. **Myers, M. L., S. Mathur, G.-H. Li, and M. Karmazyn.** Sodium-hydrogen exchange inhibitors improve postischaemic recovery of function in the perfused rabbit heart. *Cardiovasc. Res*. 29: 209–214, 1995.

40. **Numata, M., K. Petrecca, N. Lake, and J. Orlowski.** Identification of a mitochondrial Na^+/H^+ exchanger. *J. Biol. Chem*. 273: 6951–6959, 1998.
41. **Orchard, C. H., and J. C. Kentish.** Effects of changes of pH on the contractile function of cardiac muscle. *Am. J. Physiol*. 258 (*Cell Physiol*. 27): C967–C981, 1990.
42. **Orlowski, J.** Heterologous expression and functional properties of the amiloride high affinity (NHE-1) and low affinity (NHE-3) isoforms of the rat Na/H exchanger. *J. Biol. Chem*. 268: 16369–16377, 1993.
43. **Orlowski, J., and S. Grinstein.** Na^+/H^+ exchangers in mammalian cells. *J. Biol. Chem*. 272: 22373–22376, 1997.
44. **Orlowski, J., R. A. Kandasamy, and G. E. Shull.** Molecular cloning of putative members of the Na/H exchanger gene family. cDNA cloning, deduced amino acid sequence, and mRNA tissue expression of the rat Na/H exchanger NHE-1 and two structurally related proteins. *J. Biol. Chem*. 267: 9331–9339, 1992.
45. **Page, E., and L. P. McCallister.** Studies on the intercalated disk of rat left ventricular myocardial cells. *J. Ultrastruct. Res*. 43: 388–411, 1973.
46. **Pierce, G. N., W. C. Cole, K. Liu, H. Massaeli, T. G. Maddaford, Y. J. Chen, C. D. McPherson, S. Jain, and D. Sontag.** Modulation of cardiac performance by amiloride and several selected derivatives of amiloride. *J. Pharmacol. Exp. Ther*. 265: 1280–1291, 1993.
47. **Pierce, G. N., and H. Meng.** The role of sodium-proton exchange in ischemic/reperfusion injury in the heart. *Am. J. Cardiovasc. Pathol*. 4: 91–102, 1992.
48. **Pierce, G. N., and K. D. Philipson.** Na^+-H^+ exchange in cardiac sarcolemmal vesicles. *Biochim. Biophys. Acta* 818: 109–116, 1985.
49. **Pucéat, M., I. Korichneva, R. Cassoly, and G. Vassort.** Identification of band 3-like proteins and Cl^-/HCO_3^- exchange in isolated cardiomyocytes. *J. Biol. Chem*. 270: 1315–1322, 1995.
50. **Rotin, D., and S. Grinstein.** Impaired cell volume regulation in Na^+-H^+ exchange-deficient mutants. *Am. J. Physiol*. 257 (*Cell Physiol*. 26): C1158–C1165, 1989.
51. **Sato, R., A. Noma, Y. Kurachi, and H. Irisawa.** Effects of intracellular acidification on membrane currents in ventricular cells of the guinea pig. *Circ. Res*. 57: 553–561, 1985.
52. **Scholz, W., and U. Albus.** Na^+/H^+ exchange and its inhibition in cardiac ischemia and reperfusion. *Basic Res. Cardiol*. 88: 443–455, 1993.
53. **Scholz, W., U. Albus, L. Counillon, H. Gögelein, H.-J. Lang, W. Linz, A. Weichert, and B. A. Schölkens.** Protective effects of HOE642, a selective sodium-hydrogen exchange subtype 1 inhibitor, on cardiac ischaemia and reperfusion. *Cardiovasc. Res*. 29: 260–268, 1995.
54. **Scholz, W., U. Albus, H. J. Lang, W. Linz, P. A. Martorana, H. C. Englert, and B. A. Schölkens.** Hoe 694, a new Na^+/H^+ exchange inhibitor and its effects in cardiac ischaemia. *Br. J. Pharmacol*. 109: 562–568, 1993.
55. **Spray, D. C., R. L. White, F. Mazet, and M. V. Bennett.** Regulation of gap junctional conductance. *Am. J. Physiol*. 248 (*Heart Circ. Physiol*. 17): H753–H764, 1985.
56. **Sweadner, K. J., V. L. M. Herrera, S. Amato, A. Moellmann, D. K. Gibbons, and K. R. H. Repke.** Immunologic identification of Na^+, K^+-ATPase isoforms in myocardium: isoform change in deoxycorticosterone acetate-salt hypertension. *Circ. Res*. 74: 669–678, 1994.
57. **Tani, M., K. Shinmura, H. Hasegawa, and Y. Nakamura.** Effect of methylisobutyl amiloride on $[Na^+]_i$, reperfusion arrhythmias, and function in ischemic rat hearts. *J. Cardiovasc. Pharmacol*. 27: 794–801, 1996.
58. **Tse, C.-M., S. Levine, C. Yun, S. Brant, L. T. Counillon, J. Pouysségur, and M. Donowitz.** Structure/function studies of the epithelial isoforms of the mammalian Na^+/H^+ exchanger gene family. *J. Membr. Biol*. 135: 93–108, 1993.
59. **Tse, C.-M., A. I. Ma, V. W. Yang, A. J. M. Watson, S. Levine, M. H. Montrose, J. Potter, C. Sardet, J. Pouysségur, and M. Donowitz.** Molecular cloning and expression of a cDNA encoding the rabbit ileal villus cell basolateral membrane Na^+/H^+ exchanger. *EMBO J*. 10: 1957–1967, 1991.
60. **Vaughan-Jones, R. D.** Regulation of chloride in quiescent sheep-heart Purkinje fibres studied using intracellular chloride and pH-sensitive micro-electrodes. *J. Physiol. (Lond.)* 295: 111–137, 1979.
61. **Wakabayashi, S., M. Shigekawa, and J. Pouysségur.** Molecular physiology of vertebrate Na^+/H^+ exchangers. *Physiol. Rev*. 77: 51–74, 1997.
62. **Wallert, M. A., and O. Fröhlich.** Na^+-H^+ exchange in isolated myocytes from adult rat heart. *Am. J. Physiol*. 257 (*Cell Physiol*. 26): C207–C213, 1989.
63. **White, R. L., J. E. Doeller, V. K. Verselis, and B. A. Wittenberg.** Gap junctional conductance between pairs of ventricular myocytes is modulated synergistically by H^+ and Ca^{++}. *J. Gen. Physiol*. 95: 1061–1075, 1990.
64. **Xu, L., G. Mann, and G. Meissner.** Regulation of cardiac Ca^{2+} release channel (ryanodine receptor) by Ca^{2+}, H^+, Mg^{2+}, and adenine nucleotides under normal and simulated ischemic conditions. *Circ. Res*. 79: 1100–1109, 1996.
65. **Xue, Y. X., N. N. Aye, and K. Hashimoto.** Antiarrhythmic effects of HOE642, a novel Na^+-H^+ exchange inhibitor, on ventricular arrhythmias in animal hearts. *Eur. J. Pharmacol*. 317: 309–316, 1996.
66. **Yasutake, M., C. Ibuki, D. J. Hearse, and M. Avkiran.** Na^+/H^+ exchange and reperfusion arrhythmias: Protection by intracoronary infusion of a novel inhibitor. *Am. J. Physiol*. 267 (*Heart Circ. Physiol*. 36): H2430–H2440, 1994.
67. **Yu, F. H., G. E. Shull, and J. Orlowski.** Functional properties of the rat Na/H exchanger NHE-2 isoform expressed in Na/H exchanger-deficient Chinese hamster ovary cells. *J. Biol. Chem*. 268: 25536–25541, 1993.
68. **Zhang, J. F., and S. A. Siegelbaum.** Effects of external protons on single cardiac sodium channels from guinea pig ventricular myocytes. *J. Gen. Physiol*. 98: 1065–1083, 1991.